

Vibrational signature of broken chemical order in a GeS₂ glass: a molecular dynamics simulation

Sébastien Blaineau and Philippe Jund

Laboratoire de Physicochimie de la Matière Condensée , Université Montpellier 2,
Place E. Bataillon, Case 03, 34095 Montpellier, France

Abstract. Using density functional molecular dynamics simulations, we analyze the broken chemical order in a GeS₂ glass and its impact on the dynamical properties of the glass through the in-depth study of the vibrational eigenvectors. We find homopolar bonds and the frequencies of the corresponding modes are in agreement with experimental data. Localized S-S modes and 3-fold coordinated sulfur atoms are found to be at the origin of specific Raman peaks whose origin was not previously clear. Through the ring size statistics we find, during the glass formation, a conversion of 3-membered rings into larger units but also into 2-membered rings whose vibrational signature is in agreement with experiments.

PACS numbers: PACS numbers: 61.43.Bn,61.43.Fs,71.15.Pd,63.50.+x

1. INTRODUCTION

Dynamical properties of germanium disulfide glasses have been extensively studied in the last two decades using Raman and InfraRed (IR) spectroscopy [1, 2, 3, 4, 5, 6]. However, the analysis of these experimental results can be extremely complicated and the determination of the origin of the vibrational modes observed in Raman and IR spectra can therefore be hypothetical [4, 5, 6]. Theoretical calculations based on molecular dynamics simulations can be a very interesting tool in order to eliminate these uncertainties since they allow the atomic displacements at the origin of each vibrational mode to be investigated. However, the importance of charge transfers in chalcogenide glasses [7] such as GeS₂ requires the use of an *ab-initio* model which can be extremely costly in time if the size of the system is not relatively small. In a previous study we have investigated a glassy GeS₂ sample containing 96 particles [8], using a non self-consistent *ab-initio* code based on the Sankey-Niklewski scheme called FIREBALL [9]. The good agreement of the results with the available experimental data showed the excellent quality of this model for the study of chalcogenide systems. However, the relative small size of the sample did not allow a great variety of structural defects inherent to amorphous systems and made a statistical determination of the broken chemical order in g-GeS₂ difficult. Experimental spectroscopic studies of these glasses [4] have shown in addition that the structural disorder manifests itself clearly in the vibrational properties of germanium disulfide glasses and it is therefore interesting to directly investigate the origin of the corresponding vibrational modes.

Here we propose a study of a larger sample (258 particles) of glassy GeS₂ using the same model, in order to study the statistics of the broken chemical order of these materials, and to analyze in detail the vibrational properties of amorphous GeS₂ at ambient temperature. In section II we will briefly present the model which has been used (more details can be found in the original paper [9]). Subsequently, we will describe the structural disorder of our amorphous sample at short- and medium-range in section III. In section IV we will present a detailed study of the vibrational properties of the system in order to understand which atomic displacements are responsible of the modes present in the Vibrational Density of States (VDOS). Finally in section V we will summarize the major conclusions of our work.

2. MODEL

The code we have used is a first-principles type molecular-dynamics program called FIREBALL96, which is based on the local orbital electronic structure method developed by Sankey and Niklewski [10]. The foundations of this model are Density Functional Theory (DFT) [11] within the Local Density Approximation (LDA) [12], and the non-local pseudopotential scheme [13]. The use of the non-self-consistent Harris functional [14], with a set of four atomic orbitals (1s and 3p) per site that vanish

outside a cut-off radius of $5a_0$ (2.645 Å) considerably reduces the CPU time.

As said earlier, this model has given excellent results for many different chalcogenide systems over the last ten years [8, 15, 16]. In the present work, we have melted a α - GeS_2 crystal containing 258 atoms in a cubic cell of 19.21 Å at 2000K for 60 ps (24000 timesteps) in order to obtain an equilibrium liquid system (standard periodic boundary conditions have been used). We have then quenched our sample at a quenching rate of 6.8×10^{14} K/s through the glass transition (the simulated glass transition temperature is close to 1200 K). Finally we have relaxed this system at ambient temperature for 600 ps. The results shown in this article have been averaged over this period.

3. STRUCTURAL DISORDER

The broken chemical order of amorphous systems can be revealed through a detailed study of short- and medium-range order in the structure of the sample. The study of the radial pair correlation function $g(r)$ defined as

$$g(r)_{\alpha-\beta} = \frac{V}{4\pi r^2 N_\alpha} \frac{dn_\beta}{dr} \quad (1)$$

for a given $\alpha - \beta$ pair, is a standard way in order to reveal the existence of bond defects in glassy samples. We report in Fig.1 the results obtained for pairs of the same nature: Ge-Ge and S-S. The peaks corresponding to second neighbour distances, at 3.64 Å for S-S pairs, and at 2.91 Å and 3.41 Å for Ge-Ge pairs (depending of whether the intertetrahedral connections are edge or corner-sharing), have already been analyzed in our previous work on the small sample [8] (in addition to the $g(r)$ for the Ge-S pairs that does not change significantly in the large sample). However in the 258-particle sample, we observe in both graphs a small peak at short distances (2.42 Å for Ge-Ge pairs and 2.23 Å for S-S pairs), corresponding to nearest-neighbour bonds. These peaks indicate the presence of homopolar bonds, albeit in small quantities, in amorphous GeS_2 at ambient temperature. Several studies have been done on this topic, and recently two experimental studies have yielded conflicting results concerning the presence or not of homopolar bonds in stoichiometric glassy GeS_2 [17, 18]. Contrarily to Cai et al. who used Raman scattering [17], Petri et al. found no evidence for such bonds in g- GeS_2 in a neutron diffraction study [18]. It should be noted that the small concentration of these bonds, as we see them in our simulation, could explain why they can not be detected in the experimental structure factor since their effect is not strong enough to be clearly distinguished.

The Ge-Ge homopolar bonds appear in ethane-like units, where each germanium is linked to another germanium and to three sulfur atoms. An illustration of this kind of structural unit is shown in Fig.2(a). The S-S bonds as we see them in our simulation can appear in two ways: either one of the sulfur atom is non-bridging (linked to one germanium Fig.2(b)), or both are non-bridging (Fig.2(c)). In both cases the S-S bond length is 2.26 Å. We have found no S-S bonds containing two bridging sulfur atoms.

The structural disorder can also appear between atoms of different nature, when the number of first neighbours of a given particle is different from what we can expect in a crystal. In stoichiometric α - GeS_2 , one Ge atom is linked to four S atoms, and each S atom is linked to two Ge atoms. The “ideal” corresponding amorphous system is then a glassy network of GeS_4 tetrahedra, linked together by one or two S atoms depending on the type of connection between the tetrahedra. A tetrahedron which is involved in an edge-sharing link is called an edge-sharing tetrahedron, and their presence can be experimentally detected using high-resolution neutron diffraction measures. In our simulation we find that 46% of the tetrahedra are edge-sharing in glassy GeS_2 , which is extremely close to the experimental value of 44% determined by Bychkov et al.[6].

The broken chemical order can also be seen at short length scales through the analysis of the bond defects of the amorphous sample. If we study the sulfur atoms of our system, we find that only 68% of them are “correctly” linked to two Ge atoms (the Ge-S bond length is 2.23 Å (experiment: 2.21 Å[19])). We find that 14.53% of them are connected to only one Ge atom, and are therefore called terminal sulfur (or non-bridging). The interatomic distance becomes then smaller than usual, and reaches the value of 2.12 Å. This decrease in the bond length, whether the sulfur atoms are bridging or non-bridging has been studied experimentally and theoretically and similar results have been found [20, 21, 22].

The reduced coordination of the sulfur atoms is balanced by the presence of 13.95% of 3-fold coordinated sulfur, which are connected to three germanium atoms instead of two (Fig.2(d)). In these configurations, the bond length increases to 2.29 Å. All these values are reported in Table I.

TABLE I. First neighbours of the S atoms in a g-GeS₂ system containing 258 particles

No. of first Ge neighbours	S		
	Amount	Percentage	Bond length
1	25	14.53%	2.12 Å
2	117	68%	2.23 Å
3	24	13.95%	2.29 Å
Homopolar bonds S-S	6	3.52%	2.26 Å
Coordination number	$n_{tot}=2.005$	$n_{Ge}=1.97$	$n_S=0.035$

If we now focus on the germanium atoms, we see that 95.36% of them are found in usual GeS₄ tetrahedra, with four nearest S neighbours. Only 1.16% of the Ge atoms are involved in Ge(S_{1/2})₃ units and 1.16% in Ge(S_{1/2})₂ units. We can therefore say that the bond defects in g-GeS₂ are more specific to the sulfur atoms, since the coordination of germanium is extremely close to that of crystalline α -GeS₂. It can be seen that the Ge-S bond length increases in Ge(S_{1/2})₃ and Ge(S_{1/2})₂ units, and reaches the value of 2.43 Å (Table II).

TABLE II. First neighbours of the Ge atoms in a g-GeS₂ system containing 258 particles

No. of first neighbours S	Ge		
	Amount	Percentage	Bond length
2	1	1.16%	2.43 Å
3	1	1.16%	2.43 Å
4	82	95.36%	2.23 Å
Homopolar bonds Ge-Ge	2	2.32%	2.42 Å
Coordination number	$n_{tot}=3.953$	$n_S=3.93$	$n_{Ge}=0.023$

An alternative way to analyze the chemical order at medium range can be obtained through the ring size statistics. We define the size n of a ring as the number of germanium atoms present in the shortest *closed* path of alternating Ge-S bonds. Therefore a n -membered ring consists of $2n$ alternating Ge-S bonds. In crystalline α -GeS₂, the ring size can only be equal to 2 or 3. Their respective proportion is 1:2, which means that 33% of them are 2-membered rings and 66% of them are 3-membered rings. However, in amorphous g-GeS₂, these rings may have more variable sizes, and their statistics is a signature of medium range disorder. We report in Table III the respective amount and percentage of rings for $n=2, \dots, 8$ in our glassy sample (no n -membered ring with $n > 8$ was found in our 258-particles system).

We note that the percentage of 2-membered rings (38%) is extremely close to that of crystalline α -GeS₂. However, many 3-membered rings have disappeared in the amorphous structure, to become n -membered rings, with $n = 2$ and $3 < n \leq 8$. These units were probably broken during the process that led to the glassy structure, allowing for the formation of mainly larger-sized rings. To our knowledge, neither experimental results nor other simulation data have been published on the ring size statistics in g-GeS₂.

TABLE III. Ring statistics in a g-GeS₂ system containing 258 particles

Ring size	No. of rings	Percentage
2	22	38%
3	27	46.5%
4	1	1.7%
5	2	3.5%
6	2	3.5%
7	3	5.1%
8	1	1.7%

Once we can describe in detail the chemical “defects” in our glassy GeS₂ sample (with respect to the crystal), we can move on to the study of the vibrational properties of this system in order to analyze the impact of these defects on the dynamics, impact which is supposed to be important according to experimental studies [4].

4. DYNAMICAL PROPERTIES

The study of the dynamical properties of g-GeS₂ can be done through the calculation of the Vibrational Density of States (VDOS), which can be measured experimentally by inelastic neutron diffraction spectroscopy. Even though Raman and IR measurements have been performed in chalcogenide glasses, no neutron diffraction experiments have ever been performed on g-GeS₂ glasses to our knowledge. We calculate the VDOS of glassy g-GeS₂ through the diagonalization of D , the dynamical matrix of the system given by:

$$D(\phi_i, \phi_j) = \frac{\partial^2 E(\phi_i, \phi_j)}{\partial \phi_i \partial \phi_j}, \quad \phi = x, y, z \quad (2)$$

for two particles i and j . Fig.3 shows the calculated VDOS for two g-GeS₂ samples containing respectively 96 and 258 particles. In the larger sample (the topic of the present study) we notice a widening of the optical band leading to an excess of modes (compared to the small sample) between 250 and 300 cm⁻¹ and above 450 cm⁻¹. We will see later that these modes arise from structural defects that are not present in the small sample (as seen previously [8]) but in order to analyze the VDOS and to determine the nature of the atomic displacements responsible of the vibrational modes, we first calculate the Phase Quotient [23], which is defined as:

$$PQ(\omega) = \frac{\sum_m \vec{e}_m^1(\omega) \cdot \vec{e}_m^2(\omega)}{\sum_m |\vec{e}_m^1(\omega) \cdot \vec{e}_m^2(\omega)|} \quad (3)$$

where the summation is done over all first-neighbour bonds in the system. $\vec{e}_m^1(\omega)$ and $\vec{e}_m^2(\omega)$ are the eigenvectors for eigenvalue ω of the 2 particles involved in the m^{th} first-neighbour bond. If the motion of particles 1 and 2 is parallel for all first-neighbour bonds, then $PQ(\omega)$ is equal to +1. If, on the contrary, the motion is antiparallel for all pairs, then $PQ(\omega)$ has a value of -1. Fig.4 represents the calculated Phase Quotient for our glassy GeS₂ sample. It can be seen that the first band in the VDOS at low frequencies is caused by acoustic-like modes, in which a particle vibrates almost in phase with its first neighbours. These modes involve therefore extended interblock vibrations. The second band in the VDOS arises from optic-like modes, in which the eigenvectors of first neighbours are mostly opposed to each other, leading mainly to intrablock vibrations. This is consistent with the usual assignment of the acoustic and optic character of the two main bands in the VDOS.

Another interesting tool in the analysis of the vibrations of a system is the Stretching character S_c [24], which is defined as:

$$S_c = \frac{\sum_m (\vec{e}_m^1(\omega) - \vec{e}_m^2(\omega)) \cdot \vec{d}_m}{\sum_m |\vec{e}_m^1(\omega) - \vec{e}_m^2(\omega)|} \quad (4)$$

The summation is performed over all first neighbour links, and \vec{d}_m is the unit vector between the two particles of the m^{th} bond. The stretching character of g-GeS₂ is shown in Fig.5. We can see that at low frequencies, the vibrational modes arise from bending-like displacements, since S_c is close to 0. On the other hand, high frequency modes in the optic band can be attributed to stretching-like vibrations, in which the eigenvectors are almost parallel to the direction along the first-neighbour bonds, and S_c is close to 1.

In order to measure the localization of the modes, we calculate the participation ratio P_r [25]:

$$P_r = \frac{(\sum_{i=1}^N |\vec{e}_i(\omega)|^2)^2}{N \sum_{i=1}^N |\vec{e}_i(\omega)|^4} \quad (5)$$

where the summation is performed over the N particles of the sample. If the mode corresponding to the eigenvalue ω is delocalized and all atoms vibrate with equal amplitudes, then $P_r(\omega)$ will be close to 1. On the contrary, if the mode is strongly localized, then $P_r(\omega)$ will be close to 0. The results are shown in Fig.6(a) and we can see that the localized modes are mainly present in the zone between the acoustic and the optic bands and also at higher frequencies at the upper limit of the optic band. In this work, we will focus on these localized modes, not present in the small sample.

In order to determine which particles are involved in a given mode, we define the center of gravity $\vec{r}_g(\omega)$ of each mode of eigenvalue ω , and the corresponding ‘‘localization’’ length L [24], as

$$\vec{r}_g(\omega) = \frac{\sum_{i=1}^N \vec{r}_i |\vec{e}_i(\omega)|^2 / m_i}{\sum_{i=1}^N |\vec{e}_i(\omega)|^2 / m_i} \quad (6)$$

and

$$L(\omega) = \sqrt{\frac{\sum_{i=1}^N |\vec{r}_i - \vec{r}_g(\omega)|^2 |\vec{e}_i(\omega)|^2 / m_i}{\sum_{i=1}^N |\vec{e}_i(\omega)|^2 / m_i}} \quad (7)$$

where \vec{r}_i and m_i are respectively the position and the atomic mass of particle i . Periodic boundary conditions are of course taken into account in these calculations. The localization length (Fig.6(b)) represents the spatial localization of a given mode. It is a length beyond which the amplitude of the atomic vibrations decreases significantly. Its maximal value is half that of the box size which is in this case equal to 9.6 Å. For each eigenvalue, a sphere of radius L centered at $\vec{r}_g(\omega)$ will define the zone in which the vibration is located. All the particles present inside this sphere will be considered as involved in the vibration. This scheme will allow us to determine the atomic displacements responsible of each localized mode.

A very controversial aspect in the study of the dynamics of g- GeS_2 is the interpretation of the modes located in the range close to 250 cm^{-1} , since the origin of the peak observed in Raman spectroscopy has never been clearly understood. Experiments on Ge-enriched $\text{Ge}_x\text{S}_{1-x}$ systems, with different concentrations of germanium, have been performed and the feature at 250 cm^{-1} was found to increase with the Ge concentration [4, 6, 26]. This led to the hypothesis that this feature is due to tetrahedral units containing less than 4 sulfur atoms, such as $\text{Ge}(\text{S}_{1/2})_3$ or $\text{Ge}(\text{S}_{1/2})_2$ units [26]. In comparable studies these vibrations have been assigned to Ge-Ge homopolar bonds [27, 28], or to distorted rocksalt units [4]. This feature, at 250 cm^{-1} , was also found to increase in intensity under high pressure conditions [29]. In our simulation we find that these vibrational modes are localized around 3-fold coordinated sulfur atoms, with a corresponding localization length approximately equal to the first-neighbour distance between the central S atom and the 3 Ge first neighbours. This mode is therefore extremely localized, and the 3 Ge atoms are almost frozen in comparison to the central S that vibrates between them. This finding is consistent with all the experimental results mentioned above. Since Ge-rich systems contain more of these bond defects it can explain why the feature at 250 cm^{-1} in Raman spectra increases in Ge-rich compositions. Under high pressure conditions, where Ge-rich and S-rich zones have been proposed to appear [26], the same explanation holds.

We find that two different zones, at 200 cm^{-1} and 440 cm^{-1} , are localized around edge-sharing units (2-membered rings). The high-frequency feature, at 440 cm^{-1} , has been analyzed in several works [4, 6, 28], and its origin is indeed due to the vibrations of edge-sharing units. These modes are caused by symmetric breathing-like displacements as depicted in Fig.7(a). The other feature, at 200 cm^{-1} , which is not yet clearly understood, was found to increase in Ge-rich compositions [6]. We find that these modes are centered around edge-sharing units as well and are due to the vibrations shown in Fig.7(b). Since the concentration of edge-sharing tetrahedra increases significantly with Ge concentration [6], this could explain why this feature is more prominent in Ge-rich compositions.

The homopolar bonds (Ge-Ge and S-S) also have a contribution in the Vibrational Density of States. We find that the vibrations of ethane-like units, presenting Ge-Ge bonds, have a contribution at 270 cm^{-1} which is close to the value determined experimentally (260 cm^{-1}) [6] and theoretically (250 cm^{-1}) [28]. We find the vibrational modes containing S-S homopolar bonds at 486 cm^{-1} , which is exactly the value found in Raman experiments on sulfur-rich samples [4]. These modes have been attributed to the S-S bonds present in S_8 rings or S_n chains, which appear in S-rich compositions [2, 26, 28, 30]. However, in our stoichiometric GeS_2 glass we find no presence of these chains and the corresponding localization length of the mode (see Fig.6(b)) is extremely small ($\approx 1.5 \text{ \AA}$). We can therefore argue that the feature at 486 cm^{-1} in Raman spectra is not necessarily caused by *extended* S_8 rings or S_n chains, but exists as soon as localized S-S homopolar bonds are present. These homopolar bonds are only present in the large sample which explains why we observe in the VDOS an excess of modes around $\approx 270 \text{ cm}^{-1}$ and 486 cm^{-1} compared to the VDOS of the small system (Fig.3).

Another region has been extensively studied over the past 20 years, concerning the so-called A_1 and A_{1c} modes, at 340 cm^{-1} and 370 cm^{-1} [2, 4, 6, 28]. Their presence in Raman spectra has been determined as arising from the symmetric stretch of $\text{Ge}(\text{S}_{1/2})_4$ tetrahedra, in which the central germanium atom is frozen. The "companion" mode A_{1c} at 370 cm^{-1} has been proposed to be due to similar vibrations in edge-sharing tetrahedra. The A_1 and A_{1c} modes are mainly Raman-active, but cannot be identified clearly in the VDOS. Nevertheless since we have previously shown that in our simulation the other modes have frequencies very close to the experimental values, we have decided to analyze the modes between 340 and 370 cm^{-1} . We indeed find tetrahedral symmetric-stretching vibrations between 340 cm^{-1} and 360 cm^{-1} , as represented in Fig.8(a) We also find at 375 cm^{-1} , symmetric-stretching modes concerning edge-sharing tetrahedra, which are usually assigned to the A_{1c} modes (Fig.8(b)). In addition, many symmetric stretching vibrations of tetrahedra containing bond defects are present between the A_1 and A_{1c} zones. This can explain why the feature at 340 cm^{-1} in Raman spectra does not disappear in Ge-rich compositions [26, 4], even though the usual $\text{Ge}(\text{S}_{1/2})_4$ tetrahedral units are no longer present in such systems.

5. CONCLUSION

Using DFT based MD simulations, we have analyzed the structural disorder of a glassy GeS_2 sample containing 258 particles and its impact on the vibrational spectrum. Compared to a previous study on a smaller system [8], we find here the presence of homopolar bonds (even though in extremely small concentration) which *a priori* permits the disagreement between two recent experimental studies to be resolved [17, 18]. The signature of these bonds in the VDOS at 270 cm^{-1} and 486 cm^{-1} is in agreement with previous experimental and theoretical results. Nevertheless, the feature at 486 cm^{-1} , previously assigned to S-S vibrations in S_8 rings or S_n chains that can be found in S-rich compositions, is not necessarily due to such medium sized units, but can arise from by S-S vibrations at short distances. We also propose an alternative explanation of the feature at 250 cm^{-1} in the Raman spectrum, showing that the corresponding modes are centered around 3-fold coordinated sulfur atoms, often present in g- GeS_2 (13.95 % of the S particles in the present system). This explains the increase of this feature in Ge-rich compositions, as well as in high-pressure samples, as found experimentally.

Analyzing the ring size distribution we find that in the process leading from the crystal to the glass a large proportion of 3-membered rings disappears giving rise to larger rings and an excess of 2-membered rings. These rings manifest themselves in the vibrational properties of glassy GeS_2 , and principally 2 modes are found, at 200 cm^{-1} and 440 cm^{-1} , respectively assigned to bond-bending and bond-stretching vibrations of edge-sharing tetrahedra.

In the region experimentally assigned to the A_1 and A_{1c} modes we find, as expected, symmetric-stretch vibrations of corner and edge-sharing $\text{Ge}(\text{S}_{1/2})_4$ tetrahedra respectively, but also vibrations of tetrahedra containing bond defects which allows us to explain why these modes do not disappear in Ge-rich systems.

Acknowledgments

We thank David Drabold for providing some of the codes necessary to analyze the vibrational properties of our sample. Part of the numerical simulations were done at the ‘‘Centre Informatique National de l’Enseignement Supérieur’’ (CINES) in Montpellier.

-
- [1] R. J. Nemanich, Phys. Rev. B, **16**, 1655 (1977).
 - [2] S. Sugai, Phys. Rev. B **35**, 1345 (1987).
 - [3] M. Yamaguchi, T. Nakayama, and T. Yagi, Phys. Rev. B, **263-264**, 258-260 (1999).
 - [4] P. Boolchand, J. Grothaus, M. Tenhover, M. A. Hazle, and R. K. Grasselli, Phys. Rev. B **33**, 5421-5434 (1986).
 - [5] A. Perakis, I. P. Kotsalas, E. A. Pavlatou, and C. Raptis, Phys. Stat. Sol. (b) **211**, 421 (1999).
 - [6] E. Bychkov, M. Fourmentin, M. Miloshova and C. Benmore, ILL Millennium Symposium (Grenoble, France, April 6-7, 2001), p. 54.
 - [7] D. Foix, Phd. Thesis, Université de Pau, France (2003).
 - [8] S. Blaineau, P. Jund and D. Drabold, Phys. Rev. B **67**, 094204 (2003).
 - [9] A. A. Demkov, J. Ortega, O. F. Sankey, and M. Grumbach, Phys. Rev B **52**, 1618 (1995).
 - [10] O. F. Sankey and D. J. Niklewski, Phys. Rev. B, **40**, 3979 (1989).
 - [11] P. Hohenberg and W. Kohn, Phys. Rev **136**, B864 (1964).
 - [12] D. M. Ceperley and B. J. Alder, Phys. Rev. Lett. **45**, 566 (1980).
 - [13] G. B. Bachelet, D. R. Hamman, and M. Schluter, Phys. Rev. B **26**, 4199 (1982).
 - [14] J. Harris, Phys. Rev. B, **31**, 1770 (1985).
 - [15] M. Durandurdu, D. A. Drabold, and N. Mousseau, Phys. Rev B, **62** 15307 (2000).
 - [16] J. Li, D.A. Drabold, Phys Rev. B, **64** 104206 (2001).
 - [17] L. Cai and P. Boolchand, Philos. Mag. B **82**, 1649 (2002).
 - [18] I. Petri and P. S. Salmon, J. Non-Cryst. Solids **293-295**, 169 (2001).
 - [19] A. Ibanez, M. Bionducci, E. Philippot, L. Descôtes, R. Bellissent, J. Non-Cryst. Solids **202**, 248 (1996).
 - [20] J. Olivier-Fourcade, J. C. Jumas, M. Ribes, E. Philippot and M. Maurin, Journal of Solid State Chemistry **23**, 155 (1978).
 - [21] Z. V. Popovic, Phys. Lett. **94A**, 242 (1982).
 - [22] I. Fejes, F. Billes, Int. J. Quantum Chem. **85**, 85 (2001).
 - [23] R. J. Bell and D. C. Hibbins-Butler, J. Phys. Chem. **68**, 2926 (1964).
 - [24] M. Marinov and N. Zotov, Phys. Rev. B, **55**, 2938 (1997).
 - [25] R. J. Bell, Methods Comput. Phys. **15**, 215 (1976).
 - [26] G. Lucovsky, F. L. Galeener, R. C. Keezer, R. H. Geils, and H. A. Six, Phys. Rev. B **10**, 5134 (1974).
 - [27] G. Lucovsky, R. J. Nemanich, and F. L. Galeener, in *Proceedings of the 7th International Conference on Amorphous and Liquid Semiconductors, Edinburgh, Scotland, 1977*, edited by W. E. Spear (G. G. Stevenson, Dundee, Scotland, 1977), p.130.
 - [28] K. Jackson, A. Briley, S. Grossman, D. V. Porezag, and M. R. Pederson, Phys. Rev. B **60**, R14985 (1999).
 - [29] B. A. Weinstein and M. L. Slade, in *Optical Effects in Amorphous Semiconductors (Snowbird, Utah, 1984)*, edited by P. C. Taylor and S. G. Bishop (AIP, New York, 1984), p.457; see also B. A. Weinstein and R. Zallen, in *Light Scattering in Solids IV*, Vol. 54 of *Topics in Applied Physics*, edited by M. Cardona and G. Guntherodt (Springer, New York, 1984), p.465.
 - [30] A. Ibanez, M. Bionducci, E. Philippot, L. Descôtes, R. Bellissent, Journal of Non-Crystalline Solids **202**, 248 (1996).

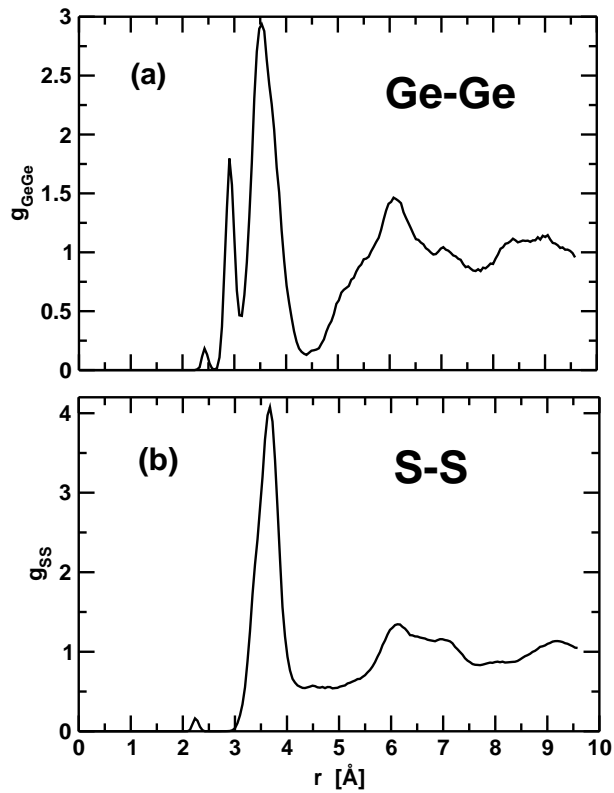
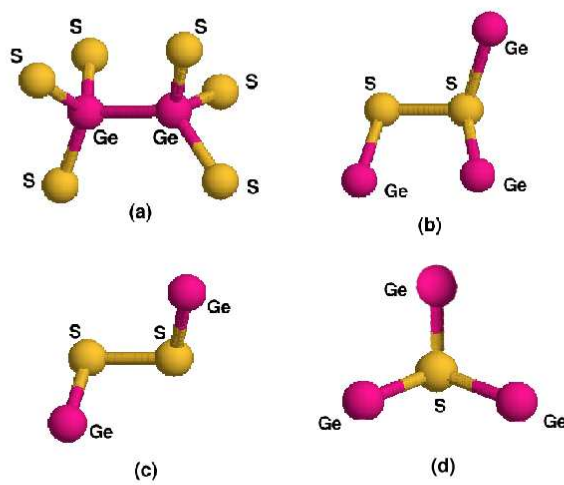
Fig 1**Figure 1.** Radial pair correlation functions for Ge-Ge (a) and S-S (b) pairs**Figure 2.** Illustration of three kind of units containing homopolar bonds: An ethane-like unit presenting a Ge-Ge homopolar bond (a), and two S-S homopolar bonds including one (b) or two (c) non-bridging Sulfur atoms. In addition a 3-coordinated sulfur atom is illustrated in (d).

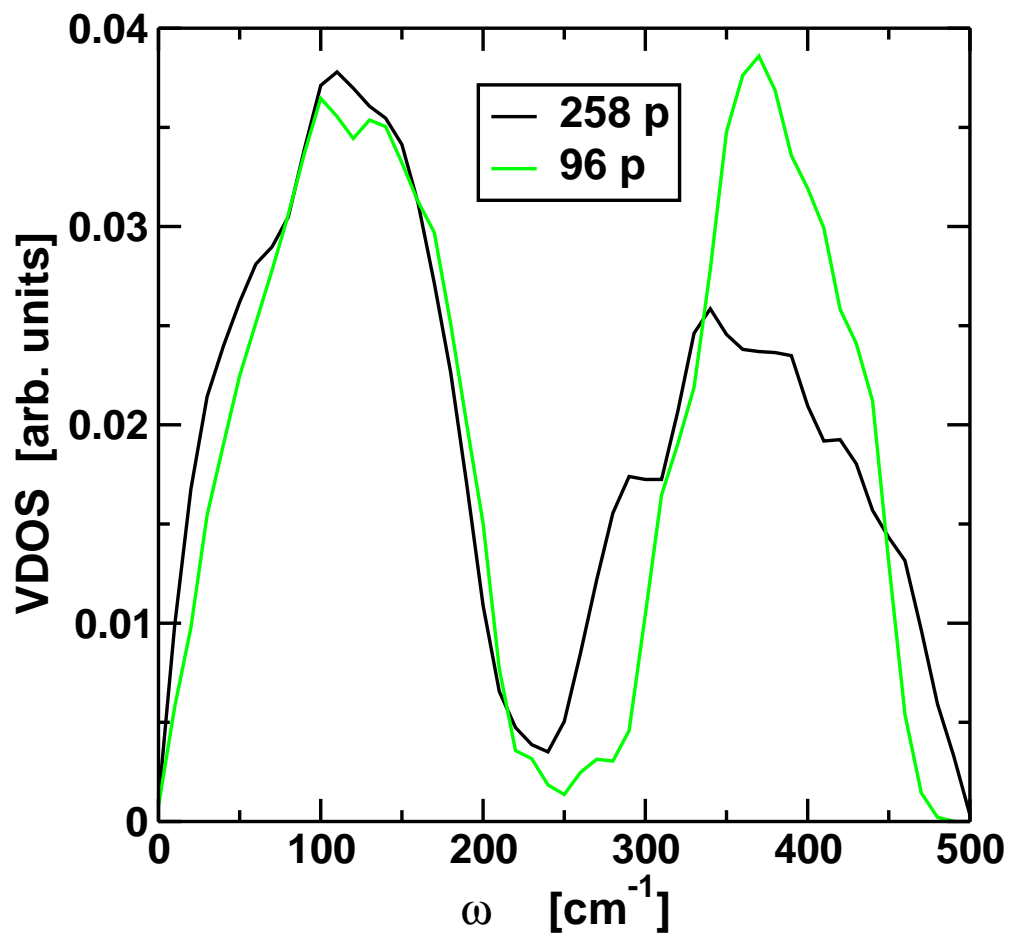
Fig 3

Figure 3. Vibrational density of states (VDOS) of the 258-particles sample compared to the one previously obtained for a 96-particle sample [8]

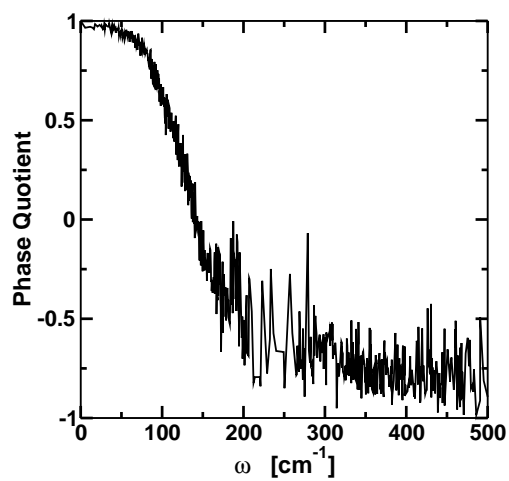
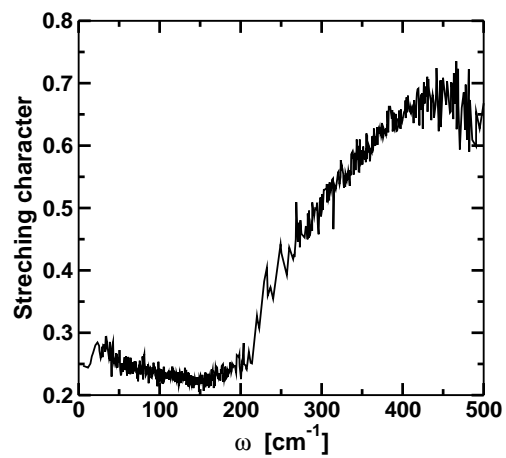
Fig 4**Figure 4.** Calculated phase quotient (see text for definition) as a function of ω **Fig 5****Figure 5.** Calculated stretching character (see text for definition) as a function of ω

Fig. 6

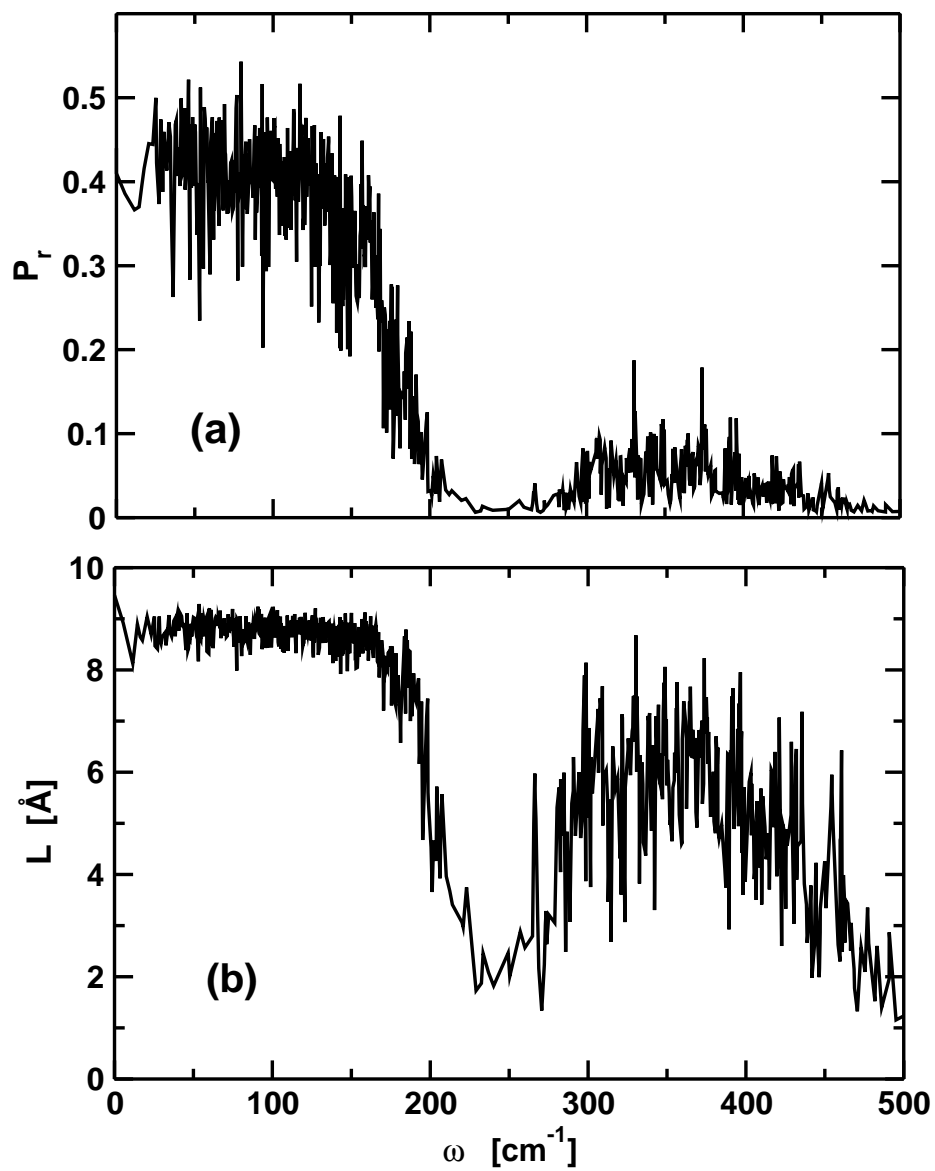


Figure 6. Calculated participation ratio (a) and localization length (b) (see text for definition) as a function of ω

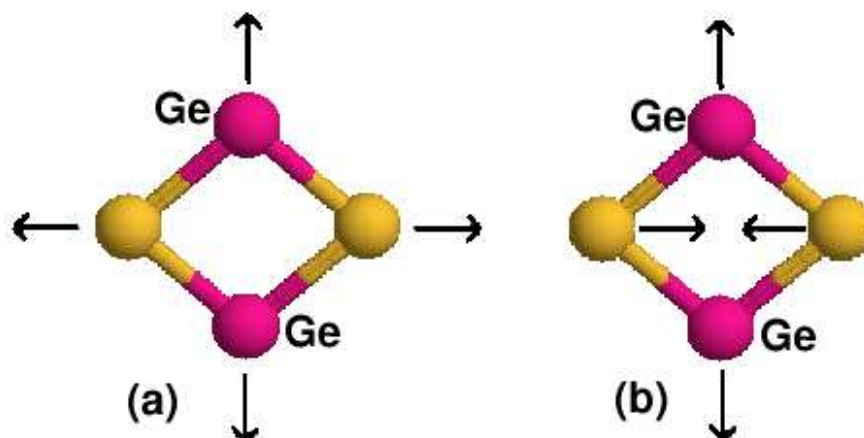


Figure 7. Atomic displacements involved in the vibrational modes at 440 cm^{-1} (a) and 200 cm^{-1} (b) concerning edge-sharing units

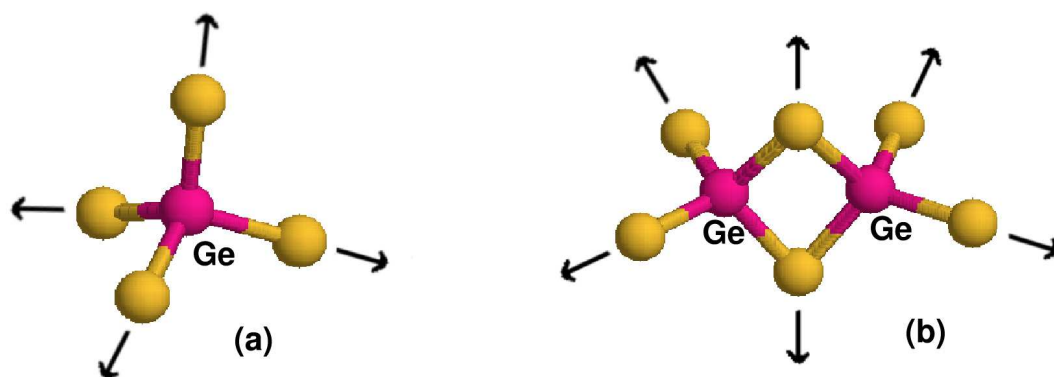


Figure 8. Atomic displacements involved in the A_1 (a) and A_{1c} (b) modes presenting symmetric-stretching vibrations of corner-sharing and edge-sharing tetrahedra